Pergamon

Solid State Communications, Vol. 108, No. 8, pp. 525–530, 1998

0038–1098/98 $ - see front matter

PII: S0038–1098(98)00396-2

DEPENDENCE OF THE PHOTOLUMINESCENCE OF Tl_2InGaS_4 LAYERED CRYSTAL ON TEMPERATURE AND EXCITATION INTENSITY

N.M. Gasanly,[a,*] A. Serpengüzel,[b] O. Gürlü,[b] A. Aydınlı[b] and İ. Yılmaz[a]

[a]Physics Department, Middle East Technical University, 06531 Ankara, Turkey
[b]Physics Department, Bilkent University, 06533 Ankara, Turkey

The emission band spectra of Tl_2InGaS_4 layered crystals were investigated in the 10–120 K temperature range and in the 540–860 nm wavelength range using photoluminescence (PL). The peak energy position of the emission band is located at 1.754 eV (707 nm) at 10 K. The emission band has a half-width of 0.28 eV and an asymmetric Gaussian lineshape. The increase of the half-width of the emission band, the blue shift of the emission band peak energy and the quenching of the PL with increasing temperature is explained using the configuration coordinate model. The blue shift of the emission band peak energy and the sublinear increase of the emission band intensity with increasing excitation intensity is explained using the inhomogenously spaced donor–acceptor pair recombination model. © 1998 Elsevier Science Ltd. All rights reserved

Keywords: A. semiconductors, D. optical properties, E. luminescence.

1. INTRODUCTION

In recent years, the III–III–VI_2 family layer-structured thallium chalcogenides such as $TlGaS_2$, $TlInS_2$ and $TlGaSe_2$ have been studied extensively [1]. At room temperature these thallium chalcogenides belong to the monoclinic system and their space group is *C2/c*. The lattice of these crystals consists of alternating two-dimensional layers arranged parallel to the (0 0 1) plane. Each successive layer is rotated by a 90° angle with respect to the previous layer.

Tl_2InGaS_4 is formed from the $TlGaS_2$–$TlInS_2$ system [2] and has an indirect band gap of 2.37 and 2.50 eV at $T = 300$ and 10 K, respectively [3]. In view of possible optoelectronic device applications in the visible region, a great deal of attention has been devoted to the study of the optical and electrical properties of these ternary thallium chalcogenides [4–6]. Long-wave optical phonons in these crystals were investigated by infrared (IR) reflection and Raman scattering experiments [7]. Recently, we have studied the photoluminescence (PL) of $TlGaS_2$ in the 10–293 K temperature range and observed three broad emission bands centered at 586, 718 and 780 nm, which we have attributed to donor-acceptor pair recombination [8].

In the present paper, we report the results of the PL investigation of Tl_2InGaS_4 single crystals in the 540–860 nm wavelength and in the 10–120 K temperature range. The shift of the emission band peak energy as well as the change of the half-width of the emission band with temperature and excitation laser intensity were also studied. The observed results were analyzed using the configurational coordinate (CC) and the inhomogenously spaced donor–acceptor pair models.

2. EXPERIMENTAL

Tl_2InGaS_4 polycrystals were synthesized from high-purity elements (at least 99.999% pure) prepared in stoichiometric proportions. Single crystals of Tl_2InGaS_4 were grown by the modified Bridgman method. The analysis of X-ray diffraction data showed that, Tl_2InGaS_4 crystallizes in a monoclinic unit cell with lattice parameters: $\mathbf{a} = 1.0639$, $\mathbf{b} = 1.0441$ and $\mathbf{c} = 1.5334$ nm and $\beta = 100.12°$. The samples were prepared by cleaving an ingot parallel to the crystal layer, which was

* Corresponding author. On leave from Physics Department, Baku State University, Baku, Azerbaijan.

perpendicular to the *c*-axis with typical sample dimensions of $4 \times 3 \times 0.7$ mm^3. The electrical conductivity of the studied samples was *p*-type as determined by the hot probe method. A ''Spectra-Physics'' argon ion laser operating at a wavelength 476.5 nm was used as the excitation source. The PL was observed from the laser illuminated face of the samples, in a direction close to the normal of the (0 0 1) plane. A ''CTI-Cryogenics M-22'' closed-cycle helium cryostat was used to cool the crystals from room temperature down to 10 K. The temperature was controlled within an accuracy of 0.5 K. The PL spectra in the 540–860 nm wavelength range were analyzed using a ''U-1000 Jobin-Yvon'' double grating spectrometer and a cooled GaAs photomultiplier equipped with the necessary photon counting electronics. A set of neutral-density filters was used to adjust the excitation laser intensity from 0.11 to 17.9 W cm^{-2}. This excitation laser intensity is the mean value of the laser intensity over the Gaussian profile.

3. RESULTS AND DISCUSSION

Figure 1 shows the PL spectra of the Tl_2InGaS_4 crystal measured in the 540–860 nm wavelength and in the 10–120 K temperature range at a constant excitation laser intensity of 11 W cm^{-2}. We observed one broad band centered at 707 nm ($h\nu_p = 1.754$ eV) in the PL spectrum at 10 K. The emission band intensity and peak position changed with respect to temperature. The emission band has a half-width of 0.28 eV with an asymmetric Gaussian lineshape. These features are typical of emission bands, which are due to donor–acceptor pair transitions observed in ternary semiconductors [9].

The intensity variation of the maximum of the emission band with respect to temperature is plotted in Fig. 2. In the 10–40 K range, the PL intensity changes very little. Above 40 K the PL intensity decreases at a larger rate, until it is dominated by a quenching process above 60 K. The activation energy ΔE for this thermal quenching process is found to be 0.062 eV. This is derived in the 65–120 K temperature range using a nonlinear least squares fit to the following equation

$$I = K \exp(\Delta E/k_B T), \tag{1}$$

where I is the PL emission intensity, K a proportionality constant and k_B the Boltzmann's constant.

Figure 3 presents the temperature dependence of the PL half-width W, which appears to follow the CC model equation [10]

$$W = W_0\{\coth(h\nu_e/2kT)\}^{1/2}, \tag{2}$$

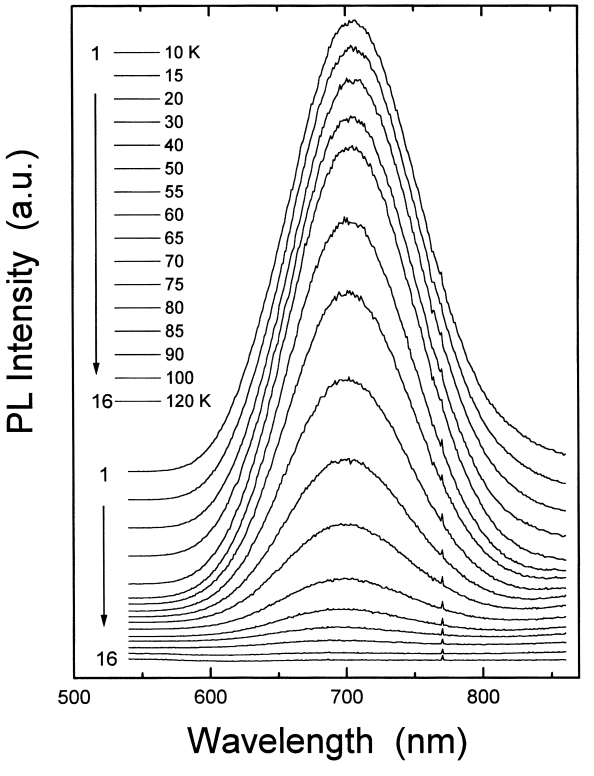

Fig. 1. PL spectra of Tl_2InGaS_4 in the 10–120 K temperature range. Excitation laser intensity $L = 11$ W cm^{-2}.

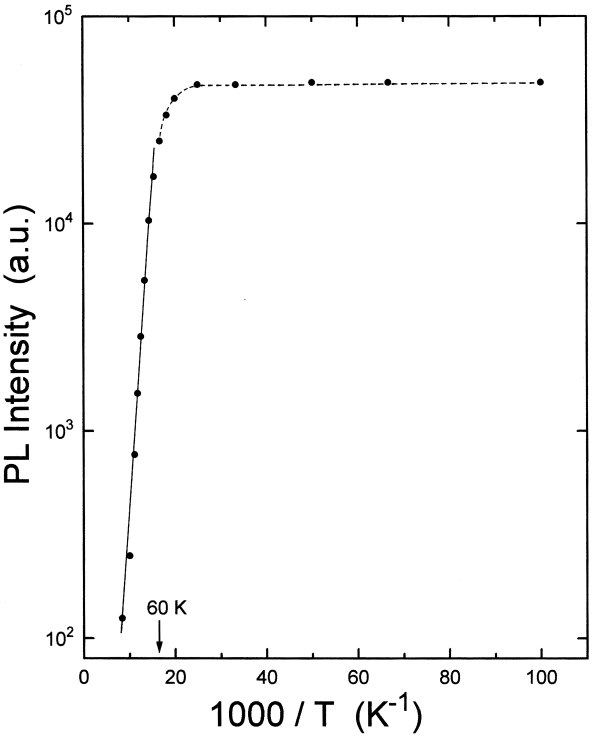

Fig. 2. Temperature dependence of Tl_2InGaS_4 PL intensity at the emission band maximum. The arrow shows the starting point of the quenching process.

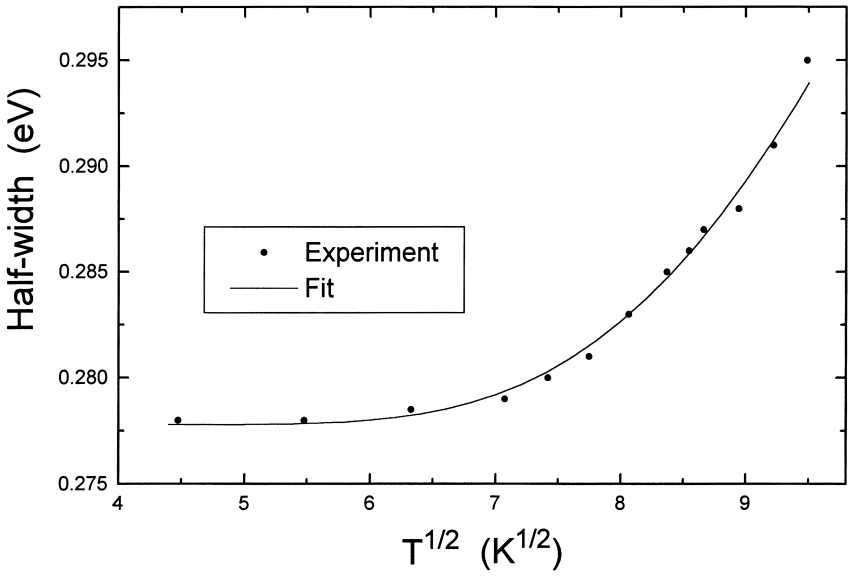

Fig. 3. Variation of the half-width with square root of temperature for Tl_2InGaS_4 emission band. The solid line is a plot of equation (2) with $h\nu_e = 0.022$ eV.

where W_0 is a constant, whose value is equal to W as the temperature approaches 0 K and $h\nu_e$ is the energy of the vibrational mode of the excited state. The half-width measurements were not performed above 90 K, because of the reduced PL intensity. However, the changes in the half-width between 10 and 90 K is large enough to show the functional dependence of equation (2). The solid line in Fig. 3 is a plot of equation (2) with parameters $W_0 = 0.278$ eV and $h\nu_e = 0.022$ eV. The fact that the excited state vibrational energy ($h\nu_e$) is lower than the LO phonon energy of 0.037 eV, measured by IR reflection [7], shows the localized nature of the centers and the validity of applying the CC model [11].

Figure 4 shows the shift of the emission peak energy as a function of temperature. The emission band peak energy increases with increasing temperature. This is opposite to the behavior of the band gap energy shift, which decreases with increasing temperature [3]. The emission band peak energy blue shifts, slowly at first, then more rapidly and finally levels off above a temperature of 85 K. The total range of the peak energy shift is 0.02 eV. Similar behavior for the peak energy shift as

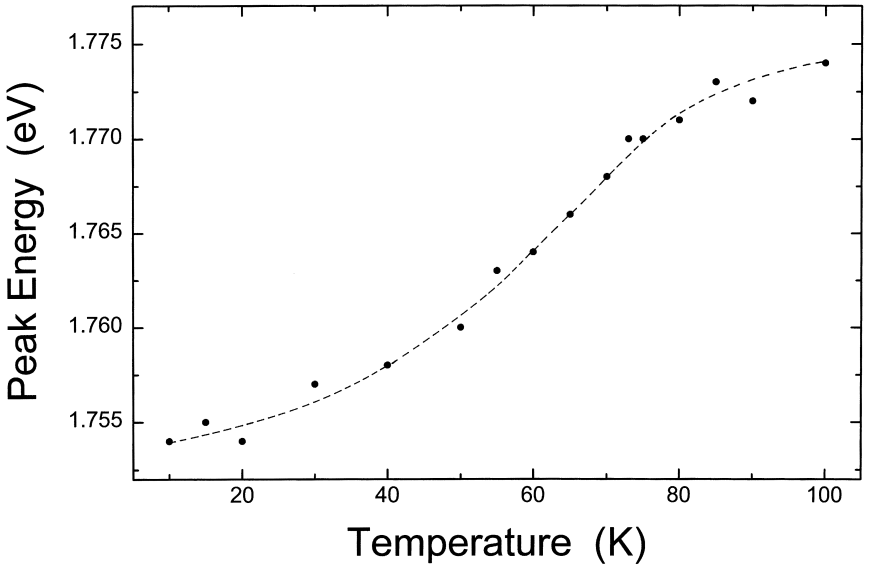

Fig. 4. Temperature dependence of Tl_2InGaS_4 emission band peak energy. The dotted line is only guide for the eye.

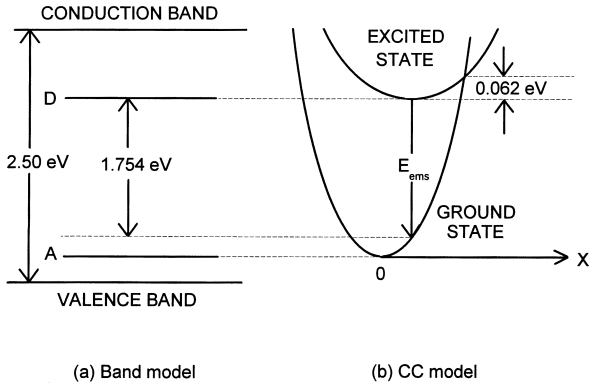

Fig. 5. Band model (a) and configurational coordinate (CC) model (b) of Tl_2InGaS_4 crystal at $T = 10$ K.

well as the above-mentioned half-width increase with temperature has been observed for the emission bands of *p*-GaAs [11] and layered *p*-GaSe [12]. The 1.37 eV (GaAs) and 1.20 eV (GaSe) emission bands were associated with a vacancy–acceptor complex center and the recombination mechanism was interpreted as self-activated luminescence in terms of the CC model. Since the CC model was so successful in explaining the behavior of the luminescence associated with such a localized center in layered *p*-GaSe, it was also applied here for layered Tl_2InGaS_4, which belongs to the same III–VI family as GaSe with a layered crystal structure.

Figure 5 shows the CC model for the Tl_2InGaS_4. Following the *p*-GaAs [11] and *p*-GaSe [12] works, let us assume that, the ground state of the localized center is derived from an acceptor level *A*, the excited state originates from a sulphur vacancy donor level *D* and, the zero point of both states lies within the band gap. Generally, in compound semiconductors a deviation from stoichiometry generates donors in the case of anion vacancies [13]. The acceptor level *A* above the top of the valence band may be linked, as in the case of GaSe [14], to the defects and stacking faults, which are due to the weak interlayer interactions in the studied crystals. Electron transitions from the excited state of the donor level to the ground state of the acceptor level gives rise to the PL with emitted photon energy E_{ems}. Also, according to the CC model, when the ground-state vibrational energy is larger than the excited-state vibrational energy, the peak shift of the emission band is opposite to the band gap energy shift [11].

In terms of the CC model, the observed quenching of the PL with increasing temperature (Figs 1 and 2) is due to an increased electron population of the excited state at higher displacement coordinates. These electrons then return to the ground state through nonradiative recombinations. Thus, the activation energy $\Delta E =$ 0.062 eV, obtained from the thermal quenching of the PL, is the difference in the energies of the lowest excited state and the intersection point of the excited and the ground state CC curves (Fig. 5).

The emission band peak shifts slightly towards higher energies with increasing excitation laser intensities in the 2.35–17.9 W cm^{-2} range (Fig. 6). The observed blue shift is a main characteristic of donor–acceptor pair recombination [13, 15] and is due to the separation inhomogeneity of the donor–acceptor pairs. The highest energies agree with transitions between closest pairs,

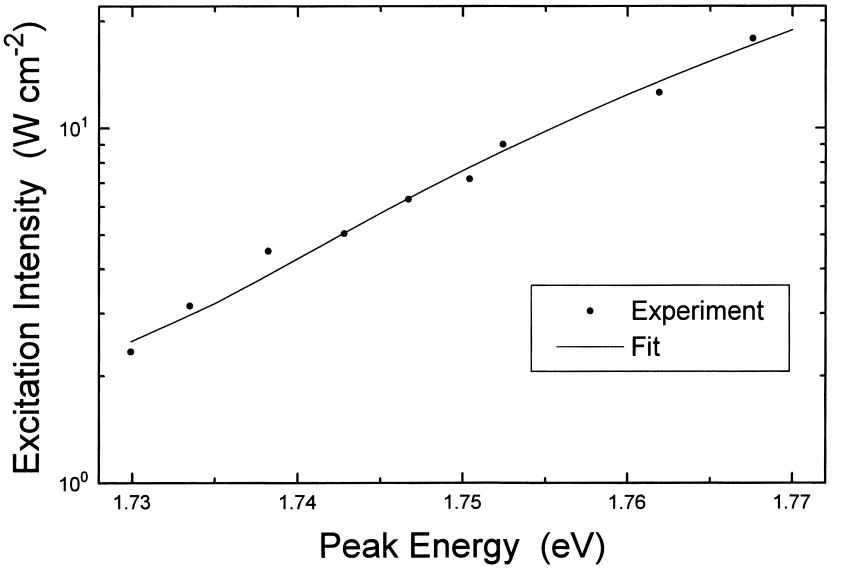

Fig. 6. Excitation laser intensity vs Tl_2InGaS_4 emission band peak energy at 10 K. The solid curve gives the theoretical fit using equation (3).

while the lowest energies correspond to pairs with large separations. For weak excitation intensities, in the 0.11–1.60 W cm^{-2} range, the emission band peak does not change its position (data not included in Fig. 6), since the number of recombination is proportional to the number of pairs, independent of the separations between the impurities [16]. For strong excitations, however, a large part of the recombination takes place at close pairs, emitting higher energy photons; the distant pairs, with small radiative transition probabilities, are saturated and cannot accommodate more carriers. The observed blue shift of 38 meV is relatively larger than that of the donor–acceptor pair bands of other binary and ternary semiconductors (e.g. 19 meV for ZnSe and 15 meV for GaP [16] and 20 meV for $CuGaSe_2$ [17]). This fact may be associated with the larger width of the donor and acceptor bands in the studied quaternary crystal than that in the binary ZnSe and GaP and in the ternary $CuGaSe_2$.

The semilog plot in Fig. 6 shows the excitation laser intensity (L) as a function of the emission band peak energy ($h\nu_p$) at 10 K. The experimental data in Fig. 6 is then fitted by the following equation [16]

$$L(h\nu_p) = L_0 \frac{(h\nu_p - h\nu_\infty)^3}{(h\nu_B + h\nu_\infty - 2h\nu_p)} \exp\left[-\frac{2(h\nu_B - h\nu_\infty)}{h\nu_p - h\nu_\infty}\right], \tag{3}$$

where L_0 is a proportionality constant, $h\nu_B$ the emitted photon energy of a close donor–acceptor pair separated by a shallow impurity Bohr radius (R_B) and $h\nu_\infty$ the emitted photon energy of an infinitely distant donor–acceptor pair. From a nonlinear least square fit of equation (3) to the experimental data, the photon energy values for an infinitely distant donor–acceptor pair and a close donor–acceptor pair separated by R_B are found to be $h\nu_\infty = 1.694$ eV and $h\nu_B = 1.754$ eV, respectively, whence $R_B = 1.59$ nm and the sum of the ionization energies of donor (E_D) and acceptor (E_A) levels is obtained to be $E_D + E_A = E_g - h\nu_\infty = 0.806$ eV at 10 K. It should be noted that, the fitted value of $h\nu_B = 1.754$ eV is less than the maximum observed PL energy peak value of $h\nu_p = 1.767$ eV (see Fig. 6). This discrepancy may be due to the fact that equation (3) was derived for binary semiconductors such as GaP and ZnSe. However, at present time there is not a more appropriate model, to our knowledge, to describe precisely the variation of the emission band peak energy as a function of the excitation laser intensity.

We have also investigated the intensity variation of the maximum of the emission band vs the excitation laser intensity at $T = 10$ K. The experimental data can be fitted by a simpler power law $I \propto L^\gamma$, where I is the PL intensity, L the excitation laser intensity and γ a dimensionless exponent. It was found that, the PL intensity increases sublinearly (i.e. $\gamma = 0.99$) with respect to the excitation laser intensity (Fig. 7). Saturation of the PL starts at $L > 7.2$ W cm^{-2}. For an excitation laser photon with an energy exceeding the band gap energy E_g, the coefficient γ is generally $1 < \gamma < 2$ for the free- and bound-exciton emission and $\gamma \leq 1$ for free-to-bound and donor–acceptor pair recombination [18]. Thus, the obtained value of $\gamma = 0.99$ confirms our assignment of the observed emission band in Tl_2InGaS_4 is due to donor–acceptor pair recombination.

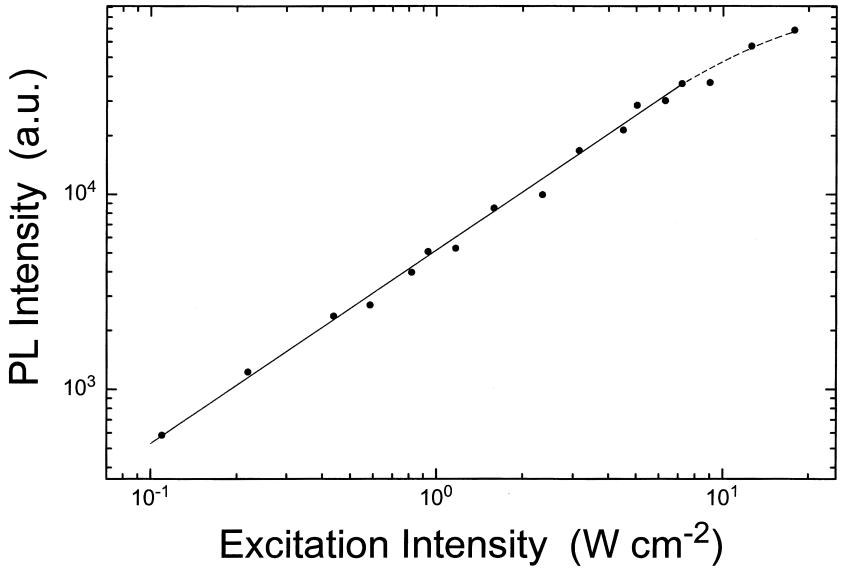

Fig. 7. Dependence of Tl_2InGaS_4 PL intensity at the emission band maximum vs excitation laser intensity at $T = 10$ K.

The analysis of the PL spectra as a function of temperature and excitation laser intensity allows one to obtain a possible model for the donor–acceptor levels located in the forbidden energy gap of the Tl_2InGaS_4 crystal. In our proposed CC model, the emission band is associated with a vacancy–acceptor complex center and the recombination mechanism is interpreted as self-activated luminescence. The excited state originates from a sulphur vacancy donor level *D*. The acceptor level *A* above the top of the valence band may be linked to defects and stacking faults in the studied layered crystals. The difference in the energies of the lowest excited state and the intersection point of the excited and the ground state CC curves is equal to the activation energy $\Delta E = 0.062$ eV, which was obtained from the thermal quenching of the PL. The blue shift of the emission band peak energy with increasing excitation laser intensity is explained using the inhomogenously spaced donor–acceptor pair model. Also, the PL intensity increases sublinearly with respect to the excitation laser intensity and confirms our assignment that the observed PL in Tl_2InGaS_4 is due to donor–acceptor pair recombination.

REFERENCES

1. Yee, K.A. and Albright, A., *J. Am. Chem. Soc*., **113,** 1991, 6474 (and references therein).
2. Bidzinova, S.M., Guseinov, G.D., Guseinov, G.G. and Zargarova, M.I., *Azerb. Khim. Zh*., **2,** 1973, 133 (in Russian).
3. Gasanly, N.M., *D. Sci. Thesis*, Baku State University, Azerbaijan, 1986 (in Russian).
4. Hanias, M.P., Anagnostopoulos, A.N., Kambas, K. and Spyridelis, J., *Mat. Res. Bull.*, **27,** 1992, 25.
5. Kalkan, N., Kalomiros, J.A., Hanias, M. and Anagnostopoulos, A.N., *Solid State Commun.*, **99,** 1996, 375.
6. Kalomiros, J.A., Kalkan, N., Hanias, M., Anagnostopoulos, A.N. and Kambas, K., *Solid State Commun.*, **96,** 1995, 601.
7. Gasanly, N.M., Goncharov, A.F., Melnik, N.N., Ragimov, A.S. and Tagirov, V.I., *Phys. Status Solidi (b)*, **116,** 1983, 427.
8. Gasanly, N.M., Aydınlı, A., Bek, A. and Yılmaz, İ, *Solid State Commun.*, **105,** 1998, 21.
9. Kim, H.G., Park, K.H., Park, B.N., Lim, H.J., Min, S.K., Park, H.L. and Kim, W.T., *Jap. J. Appl. Phys*., **32,** Suppl. No. 3, 1993, 476.
10. Willardson, R.K. and Beer, A.C., *Semiconductors and Semimetals*, Vol. 8, p. 374. Academic Press, New York, 1972.
11. Hwang, C.J., *Phys. Rev.*, **180,** 1969, 827.
12. Shigetomi, S., Ikari, T. and Nakashima, H., *J. Appl. Phys.*, **74,** 1993, 4125.
13. Pankove, J.I., *Optical Processes in Semiconductors*, p. 8 and 150. Prentice-Hall, Inc., New Jersey, 1975.
14. Capozzi, V., *Phys. Rev.*, **B28,** 1983, 4620.
15. Yu, P.Y. and Cardona, M., *Fundamentals of Semiconductors*, p. 348. Springer, Berlin, 1995.
16. Zacks, E. and Halperin, A., *Phys. Rev.*, **B6,** 1972, 3072.
17. Poure, A., Leyris, J.P. and Aicardi, J.P., *J. Phys. C: Solid State Phys.*, **14,** 1981, 521.
18. Schmidt, T., Lischka, K. and Zulehner, W., *Phys. Rev.*, **B45,** 1992, 8989.